Research on Chemical Intermediates
https://doi.org/10.1007/s11164-019-03946-6

Role of bio-derived zinc oxide nanoparticles in antifungal and photocatalytic activities

Mahsa Nourbakhsh[1] · Majid Darroudi[2,3] · Mostafa Gholizadeh[1]

Received: 20 April 2019 / Accepted: 2 August 2019

Abstract

Zinc oxide nanoparticles (ZnO-NPs) are known as a material in the treatment of environmental pollutions. In this study, ZnO-NPs were synthesized using *Boswellia mukul* gum. The characterization of synthesized ZnO-NPs was performed UV–Vis spectroscopy, powder X-ray diffraction, FTIR, and field emission scanning electron microscopy. The obtained outcomes have illustrated that the synthesized nanoparticles had been in hexagonal shapes and contained a sheet form in the size of 20–50 nm. The antifungal assay of synthesized ZnO-NPs has been studied against *Aspergillus niger* and *Aspergillus flavus*, while the minimum inhibitory concentrations of both strains have been calculated to be 18 µg/mL. We have evaluated the photocatalytic activity of synthesized ZnO-NPs through the utilization of methylene blue (MB) (Q1/R4) under UV light. The photocatalytic results of MB dye show up to 70% degradation in 180 min, which indicates that the synthesized nanoparticles are capable of deteriorating artificial colors and can eradicate some environmental contaminants.

Keywords Zinc oxide nanoparticles · *Boswellia mukul* gum · Photocatalytic · Antifungal

Introduction

Zinc oxide (ZnO) has two primary forms, including hexagonal wurtzite and cubic structures, of which wurtzite structure is most common and stable at environmental conditions [1, 2]. Zinc oxide is a semiconductor material, and it contains a band

✉ Mostafa Gholizadeh
m_gholizadeh@um.ac.ir

[1] Department of Chemistry, Faculty of Science, Ferdowsi University of Mashhad, Mashhad, Iran

[2] Nuclear Medicine Research Center, Mashhad University of Medical Sciences, Mashhad, Iran

[3] Department of Modern Sciences and Technologies, School of Medicine, Mashhad University of Medical Sciences, Mashhad, Iran

Published online: 12 August 2019

gap with the energy gap of 3.37 eV at room temperature. It has properties such as catalytic, electrical, optoelectronic, and photochemical [3, 4]. ZnO was applied in various products such as cosmetics, medicine, solar cells, rubber, and foods. Among nano-sized metal oxides, zinc oxide has been widely used due to antimicrobial and antitumor activities [5].

Zinc oxide nanoparticles (ZnO-NPs) contain a hexagonal structure that has created the ability to exhibit unique properties, including UV filtration, semiconducting, photocatalytic, anticorrosive, antifungal, and antibacterial, due to their enhancement unique surface area, decreased particle size, and increased reactivity of particle surface [6–8]; consequently, they have been applied for different applications such as sensors, solar voltaic, biomedical instruments, transducers, optics, ceramics, glass, oil, colors and pigments, and battery [9].

Many studies show that ZnO nanoparticles are potentially antibacterial against gram-positive and gram-negative bacteria [10, 11], and a several studies presented that these nanoparticles can have an excellent antifungal properties against fungal strains such as *Candida albicans* [12], *Botrytis cinerea*, *Penicillium expansum* [13], *Aspergillus flavus*, *Aspergillus nidulans*, *Trichoderma harzianum*, and *Rhizopus stolonifer* [14].

The nanoparticles of ZnO have been prepared through many different methods such as chemical vapor deposition, hydrothermal/solvothermal, microemulsion, direct deposition, sol–gel, spray pyrolysis, and RF plasma. [15, 16]. Some of these techniques are tedious or require advanced equipment and precise experimental conditions. Therefore, in the recent years, many sciences have considered and attempted to discover a satisfying and practical biosynthesis method, since it is often quite simple, affordable, reasonably renewable, and capable of producing sustainable materials [17–22].

Artificial colors have been labeled as an alarming environmental danger since they have shown resistance against degradation, and due to containing stable and complex constructions, the available conventional treatment procedures, including adsorption, ultrafiltration, coagulation, and reverse osmosis, are often unable to decolorize and mineralize them. It is quite vital to find novel procedures for eliminating these contaminants or at least converting them into innocuous products. Among the candidate methods for achieving this purpose, one would be the application of nanocatalysts, which function in the role of catalysts throughout a large variety of chemical reactions [23]. The aim of this study was improved eco-friendly method for biosynthesis of ZnO-NPs by sol–gel way using of *Boswellia mukul* gum and consider the photocatalytic influence of ZnO-NPs on removing the MB dye of an aqueous environment. The photocatalytic test results showed that methylene blue was obtained by the following optimum photocatalytic conditions: pH = 9, intervals 30 min, the amount of catalyst 10 mg, and 100 ppm methylene blue dye concentration. Under these conditions, the removal percentage of methylene blue was 70% after 180 min. In the following, the antifungal assay of synthesized ZnO-NPs against *Aspergillus niger* and *A. flavus* has been achieved and minimum inhibitory concentration (MIC) observed to be 18 µg/mL in the cases of both strains, and at the end, ZnO-NPs have been characterized by modern spectroscopy analyses [24, 25] (Q4/R2) and (Q5/R2).

Materials and methods

Biosynthesis of ZnO-NPs

To perform the synthesizing procedure of ZnO-NPs, 2.0 g of *Boswellia mukul* gum has been added to 350 mL of distilled water and stirred at 70 °C for 1 h. Then, 8.0 g of zinc nitrate has been appended to 50 mL of distilled water, and the achieved mixture has been added to the gum solution. To evaporate the solvent, we had the mixture stirred at a temperature of 80 °C. The resultant wet deposition has been dried at 110 °C for 2 h, while the obtained powder had been positioned in the furnace at 400, 500, 600, and 700 °C for 2 h. The remaining residue has been observed and confirmed to be the white powder of ZnO-NPs [7, 26] (Q6/R2).

Characterization of ZnO-NPs

The powder X-ray diffraction (PXRD) model of X'Pert PRO MPD PANalytical Company has been employed to determine the crystalline composition of the composed ZnO-NPs. We have utilized the FTIR spectrum model Tensor 27, Bruker, to ascertain the biomolecules of the synthesized sample, while the UV–Vis investigations on the nanoparticles have been performed by the employment of UV–Vis spectrophotometer model Rayleigh UV-2100. The field emission scanning electron microscopy (FESEM) of ZnO-NPs has been recorded through the application of MIRA3 TESCAN, and the biological experiments have been carried out by utilizing an Inverted Microscope model HUND, as well as a microplate reader model of Biochrom Anthos 2020 Microplate Reader.

Antifungal activity

The antifungal assay has been performed through the usage of Clinical and Laboratory Standard Institute (CLSI) (Q1/R4) in opposition to the *A. niger* and *A. flavus* strains. To be brief, we have harvested the conidial suspensions, once the isolates had been subcultured, on potato dextrose agar for 5–7 days at 35 °C, which were suspended in the normal saline that accommodated 0.025% Tween 20. After that, the inoculum has been diluted in normal saline to achieve the closing inoculum concentration of 0.4×10^4–5×10^4 CFU/mL. Later on, 900 µL of the prepared fungal suspension has been added to each well of the 96-well plate, along with 100 µL of synthesized ZnO-NPs serial dilution (0.03–32 µg/mL), separately. The minimum inhibitory concentrations (MICs), which had led to the total inhibition of fungal growth after 48 h of incubation at 35 °C, have been ascertained as the lowest drug concentration.

Photocatalytic degradation

To evaluate the photocatalytic functionality of synthesized ZnO-NPs (600 °C), 10 mg of nanoparticles has been appended to the aqueous methylene blue (MB)

solution (100 mg/L) while being shaken in a dark condition for 30 min. In the following, the appointed mixture has been placed under UV light for 3 h. Throughout different time breaks, 3 mL of the suspension has been procured and centrifuged at 4000 rpm for 5 min.

Afterward, we have scanned the supernatant solution through the usage of a UV–vis spectrophotometer. The appointed MB solution (10 mg/L) has been utilized as the control in the absence of nanoparticles. By the Beer–Lambert law, the MB concentration is precisely corresponding to the absorption, and as a result, we can calculate its degradation rate by the application of the following equation:

$$\text{Degradation}\,(\%) = \frac{A_0 - A_t}{A_0} \times 100 \tag{1}$$

where A_0 represents the absorption of the blank solution and A_t would be the absorption of the sample after t minutes of being exposed to UVA-11W light (Q7/R2).

Results and discussion

Typically, nanoparticles are known to be composed by reducing the metal ions and oxides, which is accomplished by using particular electron-donating agents, including water-soluble metal salts, hydrogen gas (H_2), borohydride salts (ABH_4), hydrazine (N_2H_4), organic acids (carboxylic acids), and other various alcohols, which are regularly toxic and costly. The performed researches have indicated that plants ingredients, involving phenolic compounds and sugars, plainly give away their electron, and this fact stands as the beginning of nanoparticles green synthesis. Therefore, we have employed the substrate of this plant throughout the synthesizing procedure of ZnO-NPs. The obtained results have suggested that the synthesizing process of ZnO-NPs had been performed quickly and contained a high purity. The UV–VIS absorption spectrum showed a broad band at 377 nm (Fig. 1) corresponds to ZnO nanoparticles at a temperature of 600 °C. This particular absorption band could have been assigned to the electron transitions from the valence band to the conduction band ($Zn_{3d} \rightarrow O_{2p}$) [27]. (Q9/R2).

We have demonstrated the PXRD patterns of synthesized ZnO-NPs are shown in Fig. 2. Every available peak has been identified with the Miller indices of (100), (002), (101), (102), (110), (103), (200), (112), (201), (004), and (202), which is probably alluded to wurtzite hexagonal ZnO with preferential orientation in (101) (JCPDS # 00-036-1451) [28]. XRD results of M. Messali et al. show hexagonal nanoparticles for their synthesized ZnO nanoparticles [29] (Q10/R2). The induced influences of calcination temperature (400, 500, 600, and 700 °C) on the synthesized nanoparticles have been evaluated as well, and the performed comparisons in between the calcination temperatures have exhibited the production of similar crystals. By enhancing the calcination temperature, we have observed an increase in the peak intensity, along with a decrease in the peak width and also increased the size of the nanoparticles, which is indicative of the crystallinity of synthesized nanoparticles [30–32] (Q9/R2).

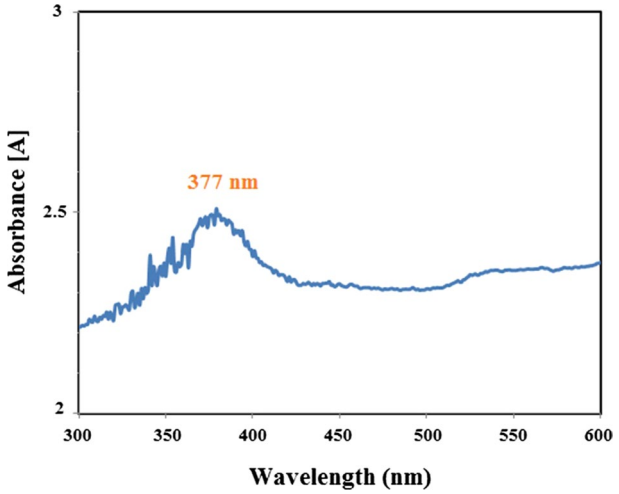

Fig. 1 UV–Vis spectrum of synthesized ZnO-NPs at 600 °C

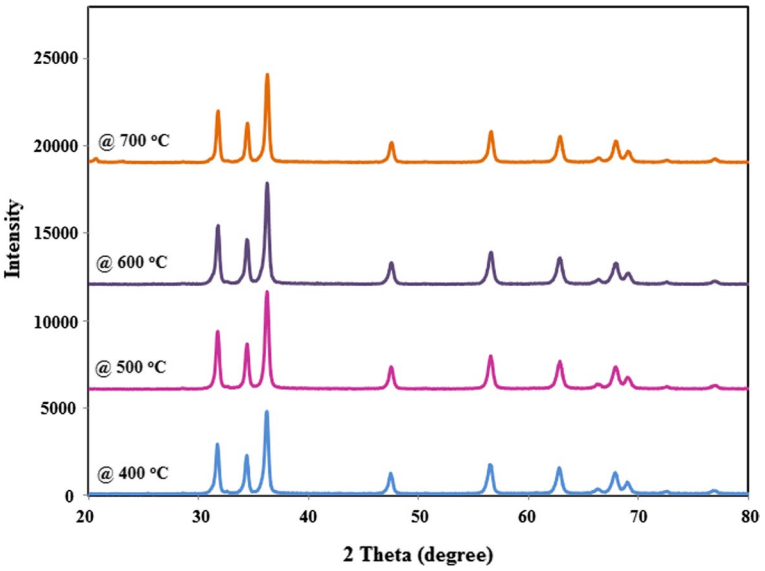

Fig. 2 PXRD diagrams of synthesized ZnO-NPs at varying temperatures

Figure 3 represents the obtained FESEM images regarding the synthesized ZnO-NPs at 400, 500, 600, and 700 °C. The hexagonal and uniformed shape ZnO particles can be perceived in the pictures, while their size has been calculated to be around 20–50 nm. FESEM images of synthesized ZnO nanoparticles by Yu et al. [33] exhibited the hexagonal structure for their nanoparticles (Q10/R2).

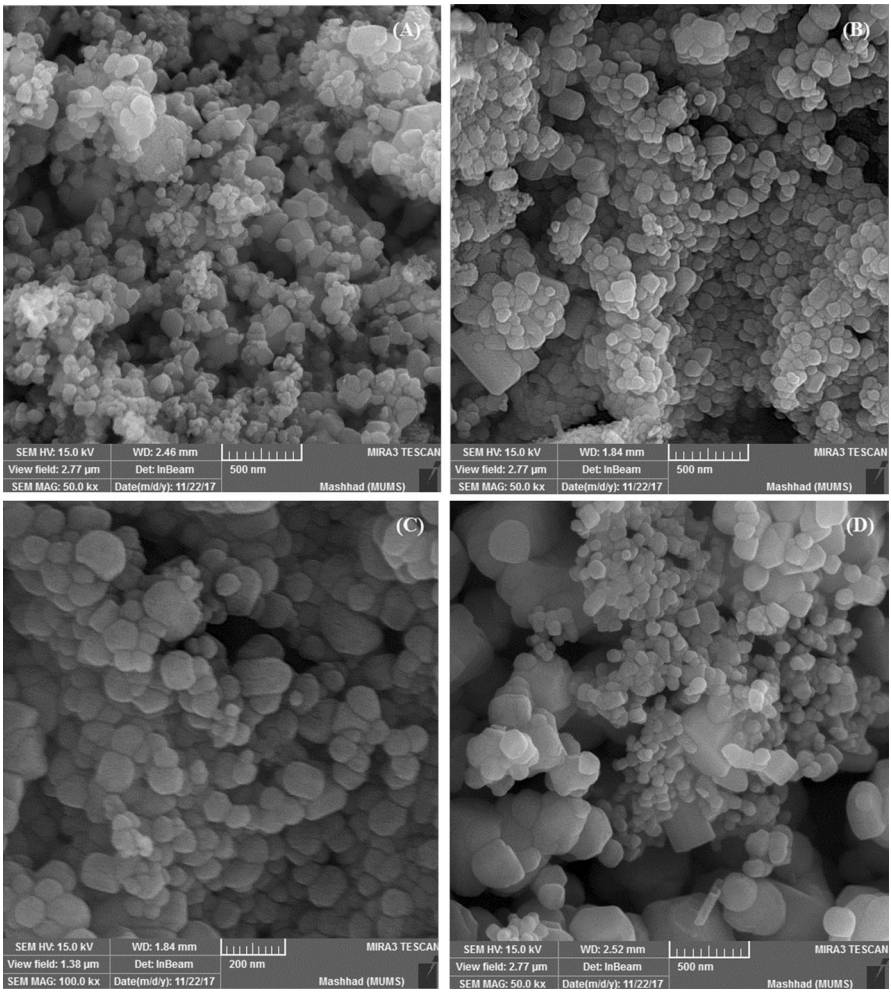

Fig. 3 FESEM images of synthesized ZnO-NPs at different temperatures, e.g., **a** 400, **b** 500, **c** 600, and **d** 700 °C

The TEM and size distribution images in Fig. 4a, b confirm a narrow size distribution and high homogeneity of prepared ZnO-NPs, which can be obtained in GT media [7] (Q12/R2).

The FTIR spectrum of synthesized ZnO-NPs has revealed a sequence of absorption peaks ranging from 400 to 4000 cm^{-1} (Fig. 5). The appearing band at 437 cm^{-1} is probably allocated to the characteristic vibrational modes of Zn–O bonding, which is indicative of the existence of ZnO-NPs. Varshney et al. [34] stated that their synthesized ZnO nanomaterials have an absorption band near 460 cm^{-1} (Q11/R2). The observed broad band at 3450 cm^{-1} is related to the O–H

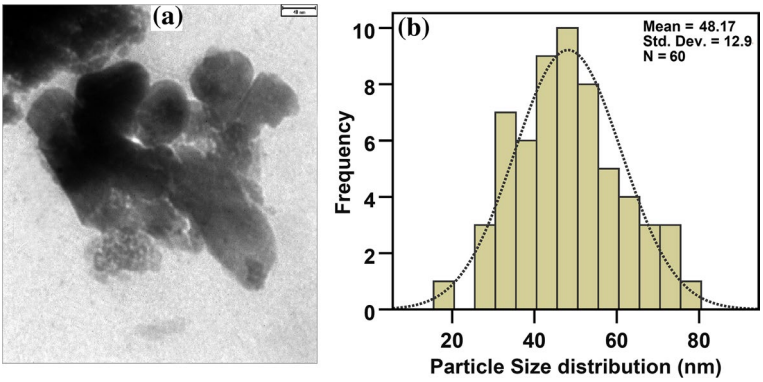

Fig. 4 TEM image (**a**) and corresponding size distribution (**b**) of synthesized ZnO-NPs at 600 °C

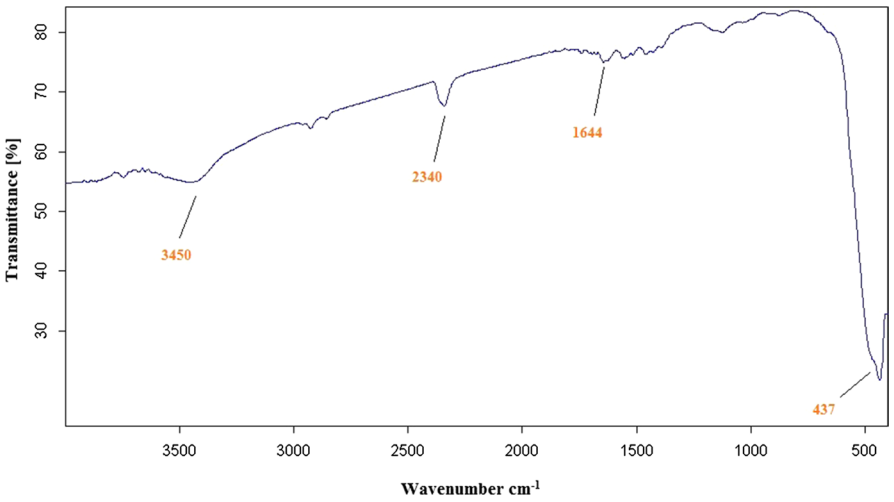

Fig. 5 FTIR spectrum of synthesized ZnO-NPs

stretching mode of water, while the existing peaks at 1644 and 1386 cm^{-1} are the resultants of asymmetrical and symmetrical stretching of carboxylate group [35].

The antifungal assay of synthesized ZnO-NPs (600 °C) has been studied against the *A. niger* and *A. flavus*, while their MICs had been calculated to be 18 µg/mL throughout the cases of both strains. One of the reasons behind the antifungal effects of ZnO-NPs maybe its attacking behavior toward the cell membrane and impairing its integrity. It is possible that a damaged cell membrane could result in the leakage of minerals, proteins, and genetic materials and consequently cause the death of cell [36].

The photocatalytic functionality of synthesized ZnO-NPs in opposition to MB, in which the time interval of UV exposure had been noted as a parameter, is shown in Fig. 6a. We have perceived the characteristic absorption peak of MB to exist within

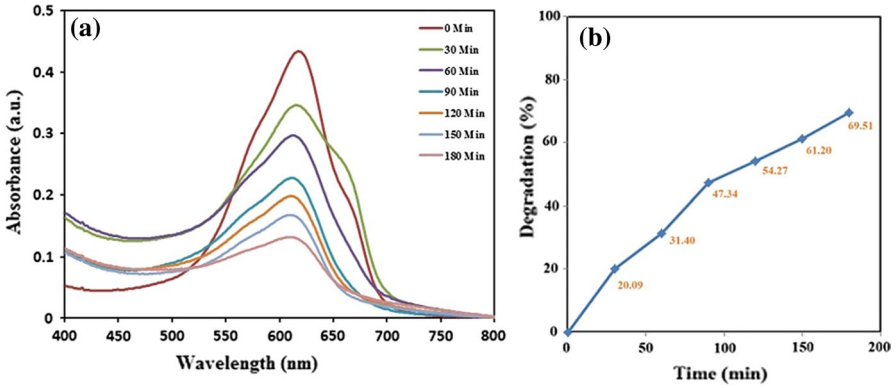

Fig. 6 **a** Absorption spectra of MB after being treated at varying time intervals and **b** the effects of irradiation time on degradation of MB in the appearance of synthesized ZnO-NPs

the range of about 630 nm (Q6/R4). While the degradation of MB has reached up to ~70% after 180 min of being exposed to light, the intensity of absorption peak had faced a reduction, and the percentage of color degradation had reached up (Fig. 6b). The control has not exhibited the inducement of any alteration in color and peak intensity throughout the experimental period.

It can be noted as a possibility that the photocatalytic qualities of ZnO-NPs in UV light are created by the excitation of SPR, while it is the responsibility of charge density oscillations to fill up the existing interface in between the phase and dielectric media. Consequently, in the role of an electron donor, ZnO-NPs are capable of altering the chemical features of color and sanitize its damaging consequences. To state outcomes of ZnO-NPs electron donation to the MB, one can note the occurrence of a decrease within the intensity of MB absorption peak. Rahman et al. [37] have investigated the photocatalytic functionality of synthesized ZnO-NPs through the usage of oxalic acid on RhB dye under UV illumination. They have reported that RhB dye has been notably degraded by ~95% within 70 min by the synthesized ZnO-NPs. In another study, Fowsiya et al. [27] *have* illustrated that the synthesized ZnO-NPs can exhibit excellent photocatalytic property on Congo red dye through the utilization of *Carissa edulis*. It has also been indicated by their review that the photocatalytic degradation of Congo red by nanoparticles had contained the rate constant of 0.4947 with 97% of degradation [27], which confirms the satisfying ability of synthesized ZnO-NPs in destroying the appointed dye.

Conclusions

Throughout this work, we have synthesized ZnO-NPs by the usage of *Boswellia mukul* gum through an inexpensive, fast, and eco-friendly method. The results have demonstrated that particles had contained a hexagonal and uniform shape, while their size has been calculated to be around 20–50 nm. The antifungal assay of synthesized ZnO-NPs against *A. niger* and *A. flavus* has been achieved and observed

to be 18 µg/mL in the cases of both strains. The performed survey on the photocatalytic activities of synthesized ZnO-NPs on MB has manifested their suitable and practical ability in destroying the color.

Acknowledgements The authors gratefully acknowledge the partial support of this study by Ferdowsi University of Mashhad Research Council (3/48910).

References

1. M. Hasanpoor, M. Aliofkhazraei, H. Delavari, Ceram. Int. **42**, 6906 (2016)
2. U. Ozgur, D. Hofstetter, H. Morkoc, Proc. IEEE **98**, 1255 (2010)
3. M. Gancheva, M. Markova-Velichkova, G. Atanasova, D. Kovacheva, I. Uzunov, R. Cukeva, Appl. Surf. Sci. **368**, 258 (2016)
4. M. Thirumavalavan, K.L. Huang, J.F. Lee, Mater. MDPI **6**, 4198 (2013)
5. P. Uikey, K. Vishwakarma, IJETCSE **21**, 239 (2016)
6. K. Elumalai, S. Velmurugan, Appl. Surf. Sci. **345**, 329 (2015)
7. M. Darroudi, Z. Sabouri, R. Kazemi Oskuee, A. Khorsand Zak, H. Kargar, M. Hasnul Naim Abd Hamid, Ceram. Int. **39**, 9195 (2013)
8. A. Singh, N.B. Singh, S. Afzal, T. Singh, I. Hussain, J. Mater. Sci. **53**, 185 (2018)
9. H. Ma, P.L. Williams, S.A. Diamond, Environ. Pollut. **172**, 76 (2013)
10. Y. Xie, Y. He, P.L. Irwin, T. Jin, X. Shi, Appl. Environ. Microbiol. **77**, 2325 (2011)
11. Z. Emami-Karvani, P. Chehrazi, Afr. J. Microbiol. Res. **5**, 1368 (2011)
12. A.A. Bazrafshan, M. Ghaedi, S. Hajati, R. Naghiha, A. Asfaram, Ecotoxicol. Environ. Saf. **142**, 330 (2017)
13. L. He, Y. Liu, A. Mustapha, M. Lin, Microbiol. Res. **166**, 207 (2011)
14. S. Gunalan, R. Sivaraj, V. Rajendran, Prog. Nat. Sci. Mater. **22**, 693 (2012)
15. W.L. Zheng, W.L. Hu, S.Y. Chen, Y. Zheng, B.H. Zhou, H.P. Wang, J. Polym. Sci. **32**, 169 (2014)
16. C.M. Ananthu, B. Renjanadevi, Proc. Technol. **24**, 761 (2016)
17. D. Suresh, P.C. Nethravathi, Udayabhanu, M.A. Pavan Kumar, H. Raja Naika, H. Nagabhushana, S.C. Sharm, Mater. Sci. Semicond. Process. **40**, 759 (2015)
18. M. Khatami, R.S. Varma, N. Zafarnia, H. Yaghoobi, M. Sarani, V.G. Kumar, Sustain. Chem. Pharm. **10**, 9 (2018)
19. A. Miri, M. Sarani, A. Hashemzadeh, Z. Mardani, M. Darroudi, Green Chem. Lett. Rev. **11**, 567 (2018)
20. H.Q. Alijani, S. Pourseyedi, M. Torkzadeh Mahani, M. Khatami, J. Mol. Struct. **1175**, 214 (2019)
21. R.K. Mishra, S. Ha, K. Verma, S.K. Tiwari, JSAMD **3**, 263 (2018)
22. S.K. Tiwari, V. Kumar, A. Huczko, R. Oraon, A. De Adhikari, G.C. Nayak, Crit. Rev. Solid State **41**, 257 (2016)
23. A. Miri, H.O. Shahraki Vahed, M. Sarani, Res. Chem. Intermed. **44**, 6907 (2018)
24. S.K. Tiwari et al., Crit. Rev. Solid State Mater. Sci. **41**, 257 (2016)
25. H. Alinezhad, F. Salehian, P. Biparva, Synth. Commun. **42**, 102 (2012)
26. M. Darroudi et al., Ceram. Int. **40**, 4827 (2014)
27. J. Fowsiya, G. Madhumitha, N.A. Al-Dhabi, M.V. Arasu, J. Photochem. Photobiol. B Biol. **162**, 395 (2016)
28. K. Rekha, M. Nirmala, M.G. Nair, A. Anukaliani, Physica B **405**, 3180 (2010)
29. M. Messali, F. Al Wadaani, H. Oudghiri-Hassani, S. Rakass, S. AlAmri, M. Benaissa, M. Abboudi, Mater. Lett. **128**, 187 (2014)
30. Z. Sabouri, A. Akbari, H. Hosseini, A. Hashemzadeh, M. Darroudi, J. Cluster Sci. 1 (2019). https://doi.org/10.1007/s10876-019-01584-x
31. Z. Sabouri, A. Akbari, H. Hosseini, A. Hashemzadeh, M. Darroudi, J. Mol. Struct. **1191**, 101 (2019)
32. M. Darroudi, Z. Sabouri, R. Kazemi Oskuee, H. Kargar, H. Hosseini, Nanomed. J. **1**, 93 (2014)
33. Z.J. Yu, M. RajeshKumar, D.L. Sun, L.T. Wang, R.Y. Hong, Mater. Lett. **166**, 284 (2016)
34. D. Varshney, K. Verma, S. Dwivedi, Optik **126**, 4232 (2015)

35. R.Y. Hong, J.H. Li, L.L. Chen, D.Q. Liu, H.Z. Li, Y. Zheng, J. Ding, Powder Technol. **189**, 426 (2009)
36. R. Wahab, M.A. Siddiqui, Q. Saquib, S. Dwivedi, J. Ahmad, J. Musarrat, A.A. Al-Khedhairy, H.S. Shin, Colloids. Surf. B Biointerfaces **117**, 267 (2014)
37. Q.I. Rahman, M. Ahmad, S.K. Misra, M. Lohani, Mater. Lett. **91**, 170 (2013)